Published in final edited form as:

Neuroimage. 2020 October 15; 220: 116991. doi:10.1016/j.neuroimage.2020.116991.

Inferior temporal tau is associated with accelerated prospective cortical thinning in clinically normal older adults

Matthew R Scott[*,1], **Olivia L Hampton**[*,1], **Rachel F Buckley**[1,2,3], **Jasmeer P Chhatwal**[1], **Bernard J Hanseeuw**[5,6], **Heidi I L Jacobs**[4,5], **Michael J Properzi**[1], **Justin S Sanchez**[5], **Keith A Johnson**[2,5], **Reisa A Sperling**[1,2], **Aaron P Schultz**[1]

[1]Department of Neurology, Massachusetts General Hospital, Harvard Medical School, Boston, MA, USA [2]Center for Alzheimer Research and Treatment, Department of Neurology, Brigham and Women's Hospital, Harvard Medical School, Boston, MA, USA [3]Melbourne School of Psychological Science, University of Melbourne, Victoria, Australia [4]Faculty of Health, Medicine and Life Sciences, School for Mental Health and Neuroscience, Alzheimer Centre Limburg, Maastricht University, Maastricht, The Netherlands [5]Division of Nuclear Medicine and Molecular Imaging, Department of Radiology, Massachusetts General Hospital, Harvard Medical School, Boston, MA, USA [6]Department of Neurology, Cliniques Universitaires Saint-Luc, Institute of Neuroscience, Université Catholique de Louvain, Brussels, Belgium

Abstract

Neurofibrillary tau tangles are a hallmark pathology of Alzheimer's disease (AD) and are more closely associated with AD-related cortical atrophy and symptom severity than amyloid-beta (Aβ). However, studies regarding the effect of tau on longitudinal cortical thinning, particularly in healthy aging and preclinical AD, have been limited in number due to the relatively recent introduction of *in vivo* PET tracers for imaging tau pathology. Here, we investigate [18F]-flortaucipir (FTP, a marker of paired helical filament tau) PET as a predictor of atrophy in healthy aging and preclinical AD. We examine longitudinal structural MRI brain imaging data, retrospectively and prospectively relative to FTP imaging, using piecewise linear mixed-effect models with time centered at each participant's FTP-PET session. Participants include 111 individuals from the Harvard Aging Brain Study who underwent at least three MRI sessions over an average of 4.46 years and one FTP-PET at the approximate midpoint of the observation period. Our primary analyses focus on inferior temporal (IT) FTP standardized uptake value ratios and longitudinal FreeSurfer defined cortical regions of interest. Relationships were also explored using other regional FTP measures (entorhinal, composite, and local), within high and low Pittsburgh

Corresponding author: Aaron P Schultz, PhD, Massachusetts General Hospital/Harvard Medical School, 149 13th Street, Suite 10.036, Charlestown, MA, United States, 02129, Phone: +1 (617) 237-0679, apschultz@mgh.harvard.edu.

*Both authors contributed equally to this work

AUTHOR CONTRIBUTIONS

MRS, OLH, and APS: Conceptualization; Data curation; Formal analysis; Methodology; Visualization

RAS and KAJ: Funding acquisition

RFB, MJP, JPC, BJH, HILJ, JSS, KAJ, and RAS: Validation

OLH and MRS: Roles/Writing - original draft

APS, OLH, MRS, RFB, MJP, JPC, BJH, HILJ, JSS, KAJ, and RAS: Writing - review & editing.

POTENTIAL CONFLICTS OF INTEREST

There are no other conflicts of interest to be reported.

compound-B (PiB) PET groups, and with longitudinal subcortical volume. Strong associations between IT FTP and cortical thinning were found, most notably in temporal, midline, and prefrontal regions, with stronger effects generally observed in the prospective as compared to retrospective time frame. Significant differences between prospective and retrospective rates of thinning were found in the inferior and middle temporal gyri, cingulate areas, as well as pars orbitalis such that higher IT FTP was associated with greater prospective rates of thinning. Within the high PiB group, significant differences between prospective and retrospective rates of thinning were similarly observed. However, no consistent pattern of tau-related change in cortical thickness within the low PiB group was discerned. These results provide support for the hypothesis that tau pathology is a driver of future atrophy as well as provide additional evidence for tau-PET as an effective AD biomarker for interventional clinical trials.

Keywords

Cortical Thinning; Tau; Longitudinal Modeling; Flortaucipir; PET; MRI; Alzheimer's Disease; Imaging

INTRODUCTION

Longstanding post-mortem studies have identified both neurofibrillary tau tangles and amyloid-beta (Aβ) plaque accumulation as hallmark pathologies of Alzheimer's disease (AD; Braak and Braak, 1991; Braak et al., 2006). Buildup of both pathologies occurs over a long prodromal period (Jack et al., 2013; Villemagne et al., 2013); however, neurofibrillary tangles are more closely associated with atrophy (Mak et al., 2018; Gordon et al., 2018), cognitive decline (Nelson et al., 2012; Maass et al., 2018), and clinical AD phenotype (Jack et al., 2018a). *In vivo* tau positron emission tomography (PET) studies have shown that tau-PET signal has strong spatial similarities to atrophy patterns (Ossenkoppele et al., 2016; Xia et al., 2017; Harrison et al., 2019; Joie et al., 2020) even before clinical AD symptoms arise (Sepulcre et al., 2016). Furthermore, tau-PET signal in these regions has been related to retrospective longitudinal cortical thinning (LaPoint et al., 2017; Gordon et al., 2018; Das et al., 2018), suggesting that atrophy occurs in temporal and spatial proximity to FTP-PET signal. However, the temporal phasing of atrophy versus tauopathy has not yet been fully demonstrated. In this study, we utilize longitudinal structural magnetic resonance imaging (MRI) as well as cross-sectional tau-PET imaging data to investigate retrospective and prospective relationships between *in vivo* flortaucipir-PET (FTP) signal and cortical thinning in clinically normal (at baseline) older adults. We use inferior temporal (IT) FTP-PET signal as a proxy for AD-related neocortical tau deposition (LaPoint et al., 2017; Sperling et al. 2019; Hanseeuw et al., 2017; Johnson et al., 2016), as the IT gyrus is an early site of tau spread into the neocortex during Braak Stage III (Braak and Braak, 1991; Braak et al., 2006), and autopsy evidence suggests that this spread from medial temporal lobe to neocortex is associated with early cognitive impairment (Braak and Braak, 1997; Hulette et al., 1998; Price and Morris, 1999). In secondary analyses we also explore effects of tau signal in three additional areas (entorhinal cortex [EC], composite, and local FTP), influences of Aβ accumulation, and bearings on subcortical volume.

We first analyze the association between longitudinal thinning over the entire observation period with cross-sectional FTP signal temporally located at the approximate midpoint of the longitudinal MR observation period. We then perform piecewise linear models to separately model retrospective and prospective rates of atrophy while maintaining a common intercept. Examining differences between retrospective and prospective effects, though not explicitly causal, can provide supporting evidence regarding whether FTP signal is more associated with retrospective atrophy, which would be consistent with tau as reflective of atrophy, or prospective atrophy, which would be consistent with tau as a driver of atrophy. This distinction is critical for understanding how to use and interpret FTP-PET as a biomarker for AD and whether tau is a good candidate target for intervention.

METHODS

Participants

Participants included 111 individuals from the Harvard Aging Brain Study (HABS), a longitudinal study of normal aging and preclinical AD conducted at Massachusetts General Hospital, Athinoula A. Martinos Center for Biomedical Imaging (Dagley et al., 2017). We refer to preclinical AD in the sense of a cognitively normal, elderly cohort that can be characterized in terms of NIA-AA criteria (Jack et al., 2018b; Sperling et al., 2011). All participants provided informed consent and were studied under protocols approved by the Partners Human Research Committee. Participants were screened for unstable medical or neurological diseases. At study entry, all participants were assessed as clinically normal (global Clinical Dementia Rating [CDR]=0, MMSE>25, and performance within 1.5 standard deviations of age and education-adjusted norms on the Logical Memory Delayed Recall), without current clinical depression (Geriatric Depression Scale<11), or active psychiatric illness (Folstein et al., 1975; Morris, 1993; Wechsler, 1987; Yesavage et al., 1982). Furthermore, participants were also excluded from the study if they had a history of alcoholism, drug abuse, or head trauma. Diagnosis was evaluated in consensus meetings using longitudinal clinical and neuropsychological assessments without regard for AD imaging biomarkers. All participants were clinically normal at the time of the FTP-PET scan.

Sample characteristics are defined in Table 1. 11 participants progressed to a global CDR of 0.5 at their latest MRI session. Neuropsychological evaluation approximately 1.5 years after each participant’s final MRI also showed a total of 20 participants progressing to a global CDR of 0.5 and 1 participant progressing to 1.0. There was an overlap of 73 participants in this sample compared to previous work on retrospective cortical thickness from HABS (LaPoint et al., 2017). The inclusion criteria for retrospective MRIs in the work of LaPoint included MRI sessions which were collected within one year following the tau-PET scan (in addition to scans before). As such, the current work included more prospective MRI sessions and classified timepoints temporally in relation to the tau-PET scan instead of labelling nearest MRI scans to the tau scan as contemporaneous. Lastly, all individuals in the current sample were required to have at least three MR sessions, which included both a retrospective and a prospective MR session relative to the tau-PET session.

Longitudinal MRI

MRI was performed on a TimTrio 3.0T imaging system (Siemens Medical Systems, Erlangen, Germany) with a 12-channel phased-array head coil over an average range of 4.46 years. Head motion was controlled with a foam pillow and extendable padded head clamps. Scanner noise was attenuated with ear plugs. Structural T1-weighted anatomical images were acquired using a magnetization-prepared rapid acquisition gradient-echo (MPRAGE; ADNI GO/2 accelerated) sequence with the following parameters: repetition time (TR)=2300 ms, echo time (TE)=2.95 ms, inversion time=900 ms, flip angle=9°, 1.05 × 1.05 × 1.2 mm resolution. However, 28 of the 386 sessions had a different sequence (ADNI GO/2 unaccelerated) with the following parameters: TR=2300 ms, TE=2.98 ms, inversion time=900 ms, flip angle=9°, 1.00 × 1.00 × 1.2 mm resolution. These sequences have been deemed equivalent. T1-weighted images were then processed with FreeSurfer version 6.0 to identify gray-white as well as pial surfaces and to produce an automatic region of interest (ROI) parcellation (Desikan et al., 2006; Fischl, 2012).

Following previously described cross-sectional quality control measures (Dagley et al., 2017), each participant's images were run through the FreeSurfer longitudinal processing stream (Reuter et al., 2012). In the longitudinal processing stream, a temporally unbiased template is created for each participant based on all MR timepoints. Next, each time point is resampled to a median template space, with the intention of reducing random variability between participant timepoints and improving the sensitivity of analyses. Identical manual quality control of FreeSurfer recons processed through the longitudinal pipeline was repeated to ensure accuracy of data, including skull stripping, white matter edits, and placement of control points in the templates and longitudinally processed scans as needed. All 34 cortical thickness ROIs produced by FreeSurfer were utilized in our analyses (Desikan-Killany). Only bihemispheric averages for each region were included in analyses as we had no *a priori* hypotheses on laterality. Effects on longitudinal lateral ventricle, inferior lateral ventricle, thalamus proper, caudate, putamen, pallidum, brain stem, hippocampus, amygdala, accumbens, cerebrospinal fluid, total gray, cortex, and ventral diencephalon volume (mm^3; based on FreeSurfer subcortical segmentation) are reported in addition to cortical ROIs.

Tau-PET Imaging

[18F]-FTP was prepared with a radiochemical yield of 14±3% and specific activity of 216±60GBq/μmol at the end of synthesis as previously reported (Johnson et al., 2016), and validated for human use (Shoup et al., 2013). Data were acquired using a Siemens/CTI ECAT HR+ scanner (3-dimensional mode, 63 image planes, 15.2 cm axial field of view, 5.6 mm trans axial resolution, and 2.4 mm slice interval), with acquisition taking place 80–100 minutes for 75 sessions and 75–105 minutes for 36 sessions, after a 9.0–11.0 mCi bolus injection in 4 × 5 minute frames for 80–100 minute sessions and 6 × 5 for 75–105 minute sessions. FTP-PET data were reconstructed as well as attenuation corrected, and each frame was evaluated to verify adequate count statistics as well as absence of head motion.

To evaluate the anatomy of cortical FTP binding, PET scans were rigidly coregistered to the individual's MPRAGE images using SPM12 (Function Imaging Laboratory, Wellcome

Department of Cognitive Neurology, London, UK). ROIs defined by the cross-sectional FreeSurfer analysis at the MRI session closest to the FTP scan were transformed into the PET native space. Reported FTP data were partial volume corrected (PVC) using the Geometric Transfer Matrix (GTM; Rousset et al., 1998) method implemented in FreeSurfer version 6.0 (Greve et al., 2016). Associations involving FTP were validated with non-PVC data. FTP signal was expressed in FreeSurfer ROIs as standardized uptake value ratios (SUVr), using cerebellar gray as the reference. Effects of a composite ROI (consisting of amygdala, fusiform, IT, middle temporal, and EC), EC, and local (i.e., both FTP and thickness measures were obtained from the same ROI) FTP are reported as supplemental information.

Amyloid-PET Imaging

Aβ-PET imaging data were acquired on average 79 days from each participant's FTP-PET visit (SD=77.80 days; median=54 days). Deposition of Aβ was measured with PET using Pittsburgh compound-B ([11C]-PiB) according to previously described methods (Johnson et al., 2007). After injection of 8.5–15.0 mCi PiB, we acquired 60 min of dynamic PET data using the Siemens/CTI ECAT HR+ PET scanner (see *Tau-PET Imaging* for parameters; 39 frames: 8×15s, 4×60s, and 27×120s). PiB-PET data were reconstructed as well as attenuation corrected, and each frame was evaluated to verify adequate count statistics as well as absence of head motion. Using Logan graphical analysis, PiB retention was expressed as a distribution volume ratio (DVR) using a cerebellar gray reference region (Price et al., 2005). Neocortical Aβ deposition was quantified using an aggregate DVR from a set of regions that comprised most of the association cortex, including frontal, lateral parietal and temporal, as well as retrosplenial cortices (FLR). Reported PiB data were PVC using the GTM method; however, PiB was only used in a secondary analysis to subset the sample into high and low Aβ subgroups. A FLR threshold of 1.34 was derived from a Gaussian mixture model on the full HABS cohort, as described by Mormino et al., 2014a. Dichotomous PVC and non-PVC classification differed by only two participants.

Statistical Analyses

Statistical analyses were performed in MATLAB R2018a (MathWorks, Inc., Natick, MA) using linear mixed-effects models with random intercepts for each participant and random time slopes. Regional bihemispheric thickness was the dependent variable in all analyses (lateral patterns are reported as supplemental material). As the purpose of the analysis is to understand atrophy with respect to FTP-PET signal, time was centered at each participant's FTP-PET visit (i.e., the time of each participant's FTP-PET session is 0). Time between the PET scan and the closest MRI scan did not significantly alter the results of our analyses. Additionally, all models included age, sex, and their interactions with time as covariates. We investigated the effect of IT FTP signal on cortical thickness over all timepoints (Table 2, Model 1). Thereafter, the effect of IT FTP on retrospective and prospective thinning was analyzed using a piecewise linear regression approach (Table 2, Model 2B). Significant differences between retrospective and prospective thickness slopes were assessed via the interaction term of IT FTP × time × observation period (i.e., retrospective vs prospective relative to the FTP scan; Table 2, Model 2A). This approach allows for both naïve modeling of non-linearities and comparisons between retrospective and prospective time periods

(relative to the FTP-PET measurement). All results are reported at a threshold of $p<0.05$, uncorrected, to investigate the pattern of these relationships across the cortex, then False Discovery Rate (FDR) corrected to confirm which associations survived adjustment for multiple comparisons. Estimates reported are not standardized. To exemplify findings, model fits of IT FTP effects on prospective and retrospective IT, EC, and cuneus thinning were generated using estimates from Model 2. Analyses were also repeated in both low and high PiB groups separately. This was done to exemplify the findings separately in healthy aging and preclinical AD cohorts as well as to avoid statistical complications and interpretability issues when modeling interactions between collinear PiB and FTP measures.

Our hypothesis is directional, such that cortical thickness is expected to decrease over time; however, as previous accounts of neuroinflammatory processes have been reported, the possibility that increases in thickness occur is not ruled out (Heneka et al., 2015; Fortea et al., 2010; Sala-Llonch et al., 2015; Weston et al., 2016). Effects across all ROIs are reported regardless of directionality. In addition to primary IT FTP analyses, we conducted additional analyses: 1) Effects of EC FTP, composite FTP, and local FTP on cortical thinning were investigated in the same manner as IT FTP. 2) We explored effects of IT FTP signal separately in high and low PiB groups to better reflect aging versus preclinical AD. 3) The associations of IT FTP signal and subcortical volume were characterized across 14 regions. Hippocampal volume is highlighted as it is a well characterized AD biomarker of brain atrophy (Huijbers et al., 2019; Hanseeuw et al., 2016; Jack et al., 1992).

RESULTS

Inferior Temporal Tau

The effect of IT FTP on longitudinal thinning across the full observation period (Model 1, IT FTP × Time; Fig. 1, Thickness Slope) was significant in sixteen regions before FDR correction and eleven regions after. Effects were observed in a variety of brain areas, however, six of the nine temporal ROIs explored had the largest effects of all 34 ROIs (in order of increasing t-statistic magnitude): EC, temporal pole, parahippocampal, fusiform, IT, and middle temporal.

For the retrospective observation period (Model 2B, IT FTP:Time:G1; Fig. 1, Retrospective Thickness Slope), higher IT FTP signal was related to faster rates of retrospective thinning in paracentral ($t(376)=-2.14$, b=−0.03, $p<0.05$) and EC regions ($t(376)=-2.58$, b=−0.05, $p<0.05$). Caudal anterior cingulate ($t(376)=2.45$, b=0.03, $p<0.05$) conversely exhibited a significant increase in retrospective thickness rates with higher IT FTP signal. However, no regions survived correction for multiple comparisons. For the prospective observation period (Model 2B, IT FTP:Time:G2; Fig. 1, Prospective Thickness Slope), higher IT FTP signal was significantly associated with faster rates of cortical thinning in eighteen regions before correction for multiple comparisons and thirteen regions following. Temporal regions were prominent, with IT ($t(376)=-4.21$, b=−0.05, $p<0.001$) and middle temporal gyri ($t(376)=-4.34$, b=−0.06, $p<0.001$) exhibiting the largest t-statistics. Cingulate regions such as the rostral anterior cingulate ($t(376)=-2.77$, b=−0.04, $p<0.01$) and posterior cingulate ($t(376)=-3.07$, b=−0.03, $p<0.01$) also showed potent effects, along with the pars orbitalis ($t(376)=-3.63$, b=−0.06, $p<0.001$).

Differences between retrospective and prospective rates of thinning (Model 2A, IT FTP × Time × G; Fig. 1, Slope Differential) were significant in IT ($t(376)=-2.04$, b=−0.04, $p<0.05$), middle temporal ($t(376)=-2.11$, b=−0.04, $p<0.05$), posterior cingulate ($t(376)=-2.19$, b=−0.03, $p<0.05$), rostral anterior cingulate ($t(376)=-2.53$, b=−0.06, $p<0.05$), and pars orbitalis ($t(376)=-2.73$, b=−0.07, $p<0.01$) such that higher IT FTP signal was associated with faster prospective thinning compared to retrospective thinning. Caudal anterior cingulate ($t(376)=-3.20$, b=−0.07, $p<0.01$) showed significantly stronger prospective thinning by IT FTP signal, driven by both significant increases in retrospective thickness and significant prospective thinning. No ROIs survived FDR correction.

T-statistics of the above analyses are displayed on brain maps in Fig. 2. These analyses were performed with non-PVC FTP data and no differences in significant ROIs (compared to PVC FTP) were observed following FDR correction. Local, EC, and composite FTP signals were analyzed in the same manner as IT FTP, and effects on cortical thinning are reported in Supplemental Fig. 1 and 2. Lateralized thickness patterns are reported in Supplemental Fig. 3. Spaghetti plots of thickness in IT, EC, caudal anterior cingulate, and cuneus across the full follow-up range and grouped by median IT FTP signal are shown in Fig. 3.

Amyloid

We repeated the above analyses separately in participants with low Aβ (putatively normal aging) and high Aβ (preclinical AD), stratified by an aggregate DVR of PiB-PET signal. Effects within each group are reported in Fig. 4. The low PiB group exhibited lower IT FTP signal than the high PiB group ($t(105)=4.89$, $p<0.001$; Table 1). In the low PiB group, significant associations between IT FTP signal and cortical thickness slopes across the full, retrospective, or prospective were only observed in the direction of increased thickness (Fig. 4A). Although we observed a significant difference in slopes in the low PiB group within IT ($t(245)=-1.97$, b=−0.07, $p<0.05$), inferior parietal ($t(245)=-2.00$, b=−0.05, $p<0.05$), parahippocampal ($t(245)=-2.03$, b=−0.09, $p<0.05$), and pericalcarine ($t(245)=2.04$, b=0.09, $p<0.05$) regions, these effects were accentuated by positive retrospective slopes that were not significantly different from 0 (except for pericalcarine). No ROIs in any low PiB analyses survived FDR correction. The high PiB group exhibited significant associations between IT FTP signal and rates of cortical thinning (Fig. 4B) in full, retrospective, or prospective periods. Retrospective increases in thickness were observed in medial orbitofrontal ($t(108)=2.02$, b=0.03, $p<0.05$) and pars orbitalis ($t(108)=2.16$, b=0.04, $p<0.05$). Rates of thinning were generally higher prospectively rather than retrospectively, with six regions demonstrating a significant difference between retrospective and prospective thinning estimates. Of these six, only the pars orbitalis survived FDR correction ($t(108)=-4.49$, b=−0.15, $p<0.001$).

Subcortical Volume

We then investigated the association between longitudinal hippocampal volume and IT FTP signal. We observed significant effects of IT FTP signal across the full follow-up ($t(378)=-2.67$, b=−39.44, $p<0.01$) and prospective period ($t(376)=-3.22$, b=−72.88, $p<0.01$), but no effect was found retrospectively. Differences between retrospective and prospective hippocampal volume rates were marginal ($t(376)=-1.83$, b=−55.13, $p=0.06$). When

separately analyzing low and high PiB groups, slope differentials were found in low PiB participants ($t(245)=-2.04$, b=−112.56, $p<0.05$) but not high PiB participants ($t(108)=0.05$, b=2.03, $p=0.96$). No significant effects were observed in either group over the full, retrospective, or prospective observation period.

Effects of IT FTP signal across subcortical ROIs are shown on brain renderings in Fig. 5. Not presented in Fig. 5, greater IT FTP signal was significantly associated with total gray ($t(378)=-2.52$, b=$-3.15\text{x}10^3$, $p<0.05$) and cortex ($t(378)=-2.77$, b=$-2.97\text{x}10^3$, $p<0.01$) atrophy over the full follow-up range, and putamen volume was marginal ($0.05<p<0.10$). Higher IT FTP signal was found to be significantly associated with prospective subcortical atrophy across the cortex ($t(376)=-3.04$, b=$-5.99\text{x}10^3$, $p<0.01$) and total gray ($t(376)=-3.29$, b=$-7.14\text{x}10^3$, $p<0.01$). At larger IT FTP levels, prospective rates of atrophy were faster than retrospective rates with total gray volume ($t(376)=-2.02$, b=$-6.22\text{x}10^3$, $p<0.05$). Brain stem, hippocampus, and thalamus exhibited marginal slope differentials ($0.05<ps<0.10$).

DISCUSSION

The present study characterized the associations of FTP-PET signal in the IT gyrus with both retrospective and prospective longitudinal cortical thinning across 34 ROIs, as well as subcortical atrophy in 14 ROIs, in a clinically normal (at baseline) sample from the Harvard Aging Brain Study. We observed that higher IT FTP signal is associated with accelerated rates of cortical thinning, and that these effects are generally stronger in prospective than retrospective observation periods. These findings are consistent with prior reports and the hypothesis that tau pathology is a driver of atrophy rather than a reflection of atrophy (Sabuncu and Konukoglu, 2014; Thompson et al., 2003; LaPoint et al., 2017; Gordon et al., 2018; Mak et al., 2018; Harrison et al., 2019).

There were widespread effects of IT FTP signal on longitudinal cortical thinning, but temporal regions were the most notable of these by surviving correction for age, sex, and multiple comparisons. Retrospective thinning was found in paracentral and EC regions. A marginal effect of the parahippocampus ($p=0.05$) was observed, which was significant in both left and right hemispheres in the previous work from HABS (LaPoint et al., 2017). Any differences in effect sizes between the current work and those found by LaPoint can be attributed to the current work's overlapping but different set of participants, characterization of retrospective MRIs (see Methods section), utilization of bihemispheric ROIs, and an updated FreeSurfer pipeline.

Prospective associations were more prevalent, with over half the ROIs exhibiting a significant prospective effect, particularly in cingulate and temporal areas. Significant differences between retrospective and prospective slopes were found in the posterior cingulate, IT gyrus, middle temporal gyrus, rostral anterior cingulate, and pars orbitalis, such that higher levels of IT FTP signal were associated with faster thinning prospectively as compared to retrospectively. These results align with prior reports highlighting temporal and medial regions as early sites for atrophy along the AD trajectory (Braak and Braak, 1991; Chan et al., 2001; Killiany et al., 2002; Scahill et al., 2002; Dickerson et al., 2009; Mormino

et al., 2014b; Mak et al., 2018; Das et al., 2018; Harrison et al., 2019). Differential slopes were also found in inferior lateral and lateral ventricles, providing further support to our cortical findings as significant volumetric increases in the ventricles could correspond to decreases in thickness or volume of neighboring areas. Moreover, we observed a p=0.06 when using hippocampal volume. Caudal anterior cingulate thickness was also found to exhibit differential rates, and its relationship was driven by a significant increase in retrospective thickness. Fig. 6 illustrates these relationships at varying levels of IT FTP in characteristic regions.

As expected, the spatial effects of EC FTP signal on longitudinal thinning were similar to that of IT FTP, which is not surprising given the high degree of collinearity between EC and IT FTP signal (r=0.83, p<0.001), and given that EC is a location of both age and AD related tauopathy (Price, 1993). Both IT and EC FTP had significant retrospective effects on EC thinning, and their prospective effects differed only slightly. Of note, we observed a strong and consistent relationship between IT FTP and EC thinning in both retrospective and prospective periods (the same pattern is true for EC FTP), which may suggest that we have missed the tipping point of the pathological cascade for the EC in the HABS sample. However, when looking at the effect of IT FTP on other medial and lateral temporal regions, we see a marked increase in the association between IT FTP signal in the prospective time frame, relative to the retrospective time frame. This may indicate that lateral temporal regions represent an inflection point in preclinical AD, and that early increases in FTP-PET signal in the IT gyrus are associated with cortical thinning in a broader AD type pattern. Analyses of local FTP signal provide additional evidence for this hypothesis, as IT thinning was the only region that exhibited a significant slope difference.

Studies of preclinical familial AD have reported an unexpected initial increase in cortical thickness, prior to later decline, indicating a potential preclinical inflammatory process (Fortea et al., 2010; Sala-Llonch et al., 2015). Though our hypothesis was directional in that we predicted increases in IT FTP to be associated with longitudinal thinning, the caudal anterior cingulate exhibited effects of IT FTP in the direction of increasing retrospective thickness. Increases in thickness were also observed in both high and low PiB groups, though low PiB effects may not be AD-related and may reflect partial volume effects. As none of these effects survived FDR correction, more work investigating early neural inflammatory processes is needed.

We ran our IT FTP models separately in individuals with high or low PiB-PET signal. In the low PiB group, we did not observe significant thinning over the full, retrospective, or prospective observation period, as only increases in thickness were observed. As expected, high PiB participants exhibited thinning effects over the full observation period, retrospectively, and prospectively. Differences between retrospective and prospective thickness were seen in both low and high PiB groups, yet these effects were largely driven by positive slopes in the retrospective time frame. Within the high PiB group, significant effects over the full and prospective period as well as significant rate differences largely mirrored the findings from the whole sample. The only regions in the high PiB individuals which varied from the full sample in differences in slopes were the IT and frontal pole. These relationships indicate that CN participants with elevated levels of both tau and

amyloid pathologies represent a heightened risk group, a finding that has been highlighted in recent prospective studies investigating cognitive trajectories within this same cohort (Sperling et al., 2019), as well as other studies investigating the association of amyloid and tau pathology to longitudinal thinning (Gordon et al., 2018; Mak et al., 2018). It should also be noted that FTP-PET and PiB-PET signals are correlated, and that high levels of IT FTP signal are rare in low PiB individuals.

There are additional limitations of the current study to consider. First, our FTP-PET measures are cross-sectional, meaning we do not know when FTP-PET signal began increasing or at what rate it is currently increasing, which means that our results are not direct evidence of a particular temporal ordering relative to atrophy and no causal inferences may be drawn directly from these results. Additional follow-up work utilizing longitudinal FTP-PET and longitudinal structural imaging is needed in both concurrent and non-overlapping time frames. Regarding effects in high amyloid versus low amyloid individuals, we must acknowledge the collinearity between PiB and FTP measurements and the general lack of IT FTP-PET signal in the low amyloid group. Additionally, as our primary analysis examined three-way interactions of time, IT FTP, and temporal grouping (Model 2), we chose not to explore four-way interactions with continuous PiB to avoid interpretation complexity. Thus, we opted to use a dichotomized PiB measure to provide more straightforward interpretability of the results. Future work could explore interactive effects of continuous PiB, as well as potential non-linearities involving PiB.

Our findings show that significant differences between retrospective and prospective rates of cortical thinning are associated with IT FTP-PET signal in AD vulnerable regions, suggesting that elevated IT FTP may be prognostic of accelerating rates of atrophy. Additional studies are needed to examine how these relationships change with longitudinal PET data, cognition, and disease progression. Our findings are consistent with the hypothesis that tau is a driving agent of cortical thinning and suggest that FTP-PET holds promise as both a biomarker for AD progression and a monitor of therapeutic effects in interventional trials.

Supplementary Material

Refer to Web version on PubMed Central for supplementary material.

ACKNOWLEDGEMENTS

We would like to acknowledge the participants of the Harvard Aging Brain Study for their dedication. This work was supported with funding from National Institutes of Health grants via R01AG027435 and for the Harvard Aging Brain Study (P01AG036694) and R01AG046396 (Dr. Johnson). This research was carried out at the Athinoula A. Martinos Center for Biomedical Imaging at the Massachusetts General Hospital, using resources provided by the Center for Functional Neuroimaging Technologies (P41EB015896), a P41 Biotechnology Resource Grant supported by the National Institute of Biomedical Imaging and Bioengineering (NIBIB), National Institutes of Health. This work also involved the use of instrumentation supported by the NIH Shared Instrumentation Grant Program and/or High-End Instrumentation Grant Program; specifically, S10RR021110, S10RR023401, S10RR019307, S10RR019254, and S10RR023043.

Dr. Schultz has received grants from the National Institute on Aging and served on paid advisory boards for Janssen Pharmaceuticals (2013) and Biogen (2016). Dr. Hanseeuw is funded by the Belgian National Fund for Scientific Research (FNRS) #SPD28094292. Dr. Jacobs reported funding from the European Union's Horizon 2020 Research and Innovation Programme under the Marie Sklodowska-Curie Grant agreement (IF-2015-GF, 706714). Dr.

Johnson has served as a paid consultant for Bayer, GE Healthcare, Janssen, Siemens Medical Solutions, Genzyme, Novartis, Biogen, Roche, AZTherapy, GEHC, Lundbeck, Genentech, Lilly/Avid, AC Immune, and Abbvie. Dr. Sperling has received grants from National Institute on Aging, Alzheimer's Association, Eli Lilly and Co., and Janssen Pharmaceuticals. She has consulted for AC Immune, Eisai, Janssen, Roche, and Takeda.

REFERENCES

Braak Heiko, and Braak Eva. "Frequency of Stages of Alzheimer-Related Lesions in Different Age Categories." Neurobiology of Aging, vol. 18, no. 4, 1997, pp. 351–357., doi:10.1016/s0197-4580(97)00056-0. [PubMed: 9330961]

Braak Heiko, and Braak Eva. "Neuropathological Stageing of Alzheimer-Related Changes." Acta Neuropathologica, vol. 82, no. 4, 1991, pp. 239–259., doi:10.1007/bf00308809. [PubMed: 1759558]

Braak Heiko, et al. "Staging of Alzheimer Disease-Associated Neurofibrillary Pathology Using Paraffin Sections and Immunocytochemistry." Acta Neuropathologica, vol. 112, no. 4, 2006, pp. 389–404., doi:10.1007/s00401-006-0127-z. [PubMed: 16906426]

Chan Dennis, et al. "Patterns of Temporal Lobe Atrophy in Semantic Dementia and Alzheimer's Disease." Annals of Neurology, vol. 49, no. 4, 2001, pp. 433–442., doi:10.1002/ana.92. [PubMed: 11310620]

Dagley Alexander, et al. "Harvard Aging Brain Study: Dataset and Accessibility." NeuroImage, vol. 144, 2017, pp. 255–258., doi:10.1016/j.neuroimage.2015.03.069. [PubMed: 25843019]

Das Sandhitsu R., et al. "Longitudinal and Cross-Sectional Structural Magnetic Resonance Imaging Correlates of AV-1451 Uptake." Neurobiology of Aging, vol. 66, 2018, pp. 49–58., doi:10.1016/j.neurobiolaging.2018.01.024. [PubMed: 29518752]

Desikan Rahul S., et al. "An Automated Labeling System for Subdividing the Human Cerebral Cortex on MRI Scans into Gyral Based Regions of Interest." NeuroImage, vol. 31, no. 3, 2006, pp. 968–980., doi:10.1016/j.neuroimage.2006.01.021. [PubMed: 16530430]

Dickerson Bradford C., et al. "The Cortical Signature of Alzheimer's Disease: Regionally Specific Cortical Thinning Relates to Symptom Severity in Very Mild to Mild AD Dementia and Is Detectable in Asymptomatic Amyloid-Positive Individuals." Cerebral Cortex, vol. 19, no. 3, 2009, pp. 497–510., doi:10.1093/cercor/bhn113. [PubMed: 18632739]

Fischl Bruce. "FreeSurfer." NeuroImage, vol. 62, no. 2, 2012, pp. 774–781., doi:10.1016/j.neuroimage.2012.01.021. [PubMed: 22248573]

Folstein Marshal F., et al. "'Mini-Mental State.'" Journal of Psychiatric Research, vol. 12, no. 3, 1975, pp. 189–198., doi:10.1016/0022-3956(75)90026-6. [PubMed: 1202204]

Fortea Juan, et al. "Increased Cortical Thickness and Caudate Volume Precede Atrophy in PSEN1 Mutation Carriers." Journal of Alzheimer's Disease, vol. 22, no. 3, 2010, pp. 909–922., doi:10.3233/jad-2010-100678.

Gordon Brian A., et al. "Cross-Sectional and Longitudinal Atrophy Is Preferentially Associated with Tau Rather than Amyloid β Positron Emission Tomography Pathology." Alzheimer's & Dementia: Diagnosis, Assessment & Disease Monitoring, vol. 10, no. 1, 2018, pp. 245–252., doi:10.1016/j.dadm.2018.02.003.

Greve Douglas N., et al. "Different Partial Volume Correction Methods Lead to Different Conclusions: An 18F-FDG-PET Study of Aging." NeuroImage, vol. 132, 2016, pp. 334–343., doi:10.1016/j.neuroimage.2016.02.042. [PubMed: 26915497]

Hanseeuw Bernard J., et al. "Decreased Hippocampal Metabolism in High-Amyloid Mild Cognitive Impairment." Alzheimer's & Dementia, vol. 12, no. 12, 2016, pp. 1288–1296., doi:10.1016/j.jalz.2016.06.2357.

Hanseeuw Bernard J., et al. "Fluorodeoxyglucose Metabolism Associated with Tau-Amyloid Interaction Predicts Memory Decline." Annals of Neurology, vol. 81, no. 4, 2017, pp. 583–596., doi:10.1002/ana.24910. [PubMed: 28253546]

Harrison Theresa M., et al. "Longitudinal Tau Accumulation and Atrophy in Aging and Alzheimer Disease." Annals of Neurology, vol. 85, no. 2, 2019, pp. 229–240., doi:10.1002/ana.25406. [PubMed: 30597624]

Heneka Michael T, et al. "Neuroinflammation in Alzheimer's Disease." The Lancet Neurology, vol. 14, no. 4, 2015, pp. 388–405., doi:10.1016/s1474-4422(15)70016-5. [PubMed: 25792098]

Huijbers Willem, et al. “Tau Accumulation in Clinically Normal Older Adults Is Associated with Hippocampal Hyperactivity.” The Journal of Neuroscience, vol. 39, no. 3, 2019, pp. 548–556., doi:10.1523/jneurosci.1397-18.2018. [PubMed: 30482786]

Hulette Christine M., et al. “Neuropathological and Neuropsychological Changes in ‘Normal’ Aging.” Journal of Neuropathology and Experimental Neurology, vol. 57, no. 12, 1998, pp. 1168–1174., doi:10.1097/00005072-199812000-00009. [PubMed: 9862640]

Jack Clifford R, et al. “MR-Based Hippocampal Volumetry in the Diagnosis of Alzheimer’s Disease.” Neurology, vol. 42, no. 1, 1992, pp. 183–183., doi:10.1212/wnl.42.1.183. [PubMed: 1734300]

Jack Clifford R, et al. “Tracking Pathophysiological Processes in Alzheimer’s Disease: an Updated Hypothetical Model of Dynamic Biomarkers.” The Lancet Neurology, vol. 12, no. 2, 2013, pp. 207–216., doi:10.1016/s1474-4422(12)70291-0. [PubMed: 23332364]

Jack Clifford R, et al. “Longitudinal Tau PET in Ageing and Alzheimer’s Disease.” Brain, vol. 141, no. 5, 2018(a), pp. 1517–1528., doi:10.1093/brain/awy059. [PubMed: 29538647]

Jack Clifford R., et al. “NIA-AA Research Framework: Toward a Biological Definition of Alzheimer’s Disease.” Alzheimer’s & Dementia, vol. 14, no. 4, 2018(b), pp. 535–562., doi:10.1016/j.jalz.2018.02.018.

Johnson Keith A., et al. “Imaging of Amyloid Burden and Distribution in Cerebral Amyloid Angiopathy.” Annals of Neurology, vol. 62, no. 3, 2007, pp. 229–234., doi:10.1002/ana.21164. [PubMed: 17683091]

Johnson Keith A., et al. “Tau Positron Emission Tomographic Imaging in Aging and Early Alzheimer Disease.” Annals of Neurology, vol. 79, no. 1, 2016, pp. 110–119., doi:10.1002/ana.24546. [PubMed: 26505746]

Joie Renaud La, et al. “Prospective Longitudinal Atrophy in Alzheimer’s Disease Correlates with the Intensity and Topography of Baseline Tau-PET.” Science Translational Medicine, vol. 12, no. 524, 2020, doi:10.1126/scitranslmed.aau5732.

Killiany RJ, et al. “MRI Measures of Entorhinal Cortex vs Hippocampus in Preclinical AD.” Neurology, vol. 58, no. 8, 2002, pp. 1188–1196., doi:10.1212/wnl.58.8.1188. [PubMed: 11971085]

LaPoint Molly R., et al. “The Association between Tau PET and Retrospective Cortical Thinning in Clinically Normal Elderly.” NeuroImage, vol. 157, 2017, pp. 612–622., doi:10.1016/j.neuroimage.2017.05.049. [PubMed: 28545932]

Maass Anne, et al. “Entorhinal Tau Pathology, Episodic Memory Decline, and Neurodegeneration in Aging.” The Journal of Neuroscience, vol. 38, no. 3, 2017, pp. 530–543., doi:10.1523/jneurosci.2028-17.2018. [PubMed: 29192126]

Mak Elijah, et al. “In Vivo Coupling of Tau Pathology and Cortical Thinning in Alzheimer’s Disease.” Alzheimer’s & Dementia: Diagnosis, Assessment & Disease Monitoring, vol. 10, no. 1, 2018, pp. 678–687., doi:10.1016/j.dadm.2018.08.005.

Mormino Elizabeth C., et al. “Amyloid and APOE 4 Interact to Influence Short-Term Decline in Preclinical Alzheimer Disease.” Neurology, vol. 82, no. 20, 2014(a), pp. 1760–1767., doi:10.1212/wnl.0000000000000431. [PubMed: 24748674]

Mormino Elizabeth C., et al. “Synergistic Effect of β-Amyloid and Neurodegeneration on Cognitive Decline in Clinically Normal Individuals.” JAMA Neurology, vol. 71, no. 11, 2014(b), p. 1379., doi:10.1001/jamaneurol.2014.2031. [PubMed: 25222039]

Morris JC “The Clinical Dementia Rating (CDR): Current Version and Scoring Rules.” Neurology, vol. 43, no. 11, 1993, pp. 2412–2412., doi:10.1212/wnl.43.11.2412-a.

Nelson Peter T., et al. “Correlation of Alzheimer Disease Neuropathologic Changes With Cognitive Status: A Review of the Literature.” Journal of Neuropathology & Experimental Neurology, vol. 71, no. 5, 2012, pp. 362–381., doi:10.1097/nen.0b013e31825018f7. [PubMed: 22487856]

Ossenkoppele Rik, et al. “Tau PET Patterns Mirror Clinical and Neuroanatomical Variability in Alzheimer’s Disease.” Brain, vol. 139, no. 5, 2016, pp. 1551–1567., doi:10.1093/brain/aww027. [PubMed: 26962052]

Price Joseph L. “The Relationship between Tangle and Plaque Formation during Healthy Aging and Mild Dementia.” Neurobiology of Aging, vol. 14, no. 6, 1993, pp. 661–663., doi:10.1016/0197-4580(93)90062-g. [PubMed: 8295678]

Price Joseph L., and Morris John C.. “Tangles and Plaques in Nondemented Aging and Preclinical Alzheimer’s Disease.” Annals of Neurology, vol. 45, no. 3, 1999, pp. 358–368., doi:10.1002/1531-8249(199903)45:33.0.co;2-x. [PubMed: 10072051]

Price Julie C., et al. “Kinetic Modeling of Amyloid Binding in Humans Using PET Imaging and Pittsburgh Compound-B.” Journal of Cerebral Blood Flow & Metabolism, vol. 25, no. 11, 2005, pp. 1528–1547., doi:10.1038/sj.jcbfm.9600146. [PubMed: 15944649]

Reuter Martin, et al. “Within-Subject Template Estimation for Unbiased Longitudinal Image Analysis.” NeuroImage, vol. 61, no. 4, 2012, pp. 1402–1418., doi:10.1016/j.neuroimage.2012.02.084. [PubMed: 22430496]

Rousset Olivier G., et al., “Correction for partial volume effects in PET: principle and validation.” Journal of Nuclear Medicine, 1998; vol. 39 no. 5, pp. 904–11. [PubMed: 9591599]

Sabuncu Mert R., and Konukoglu Ender. “Clinical Prediction from Structural Brain MRI Scans: A Large-Scale Empirical Study.” Neuroinformatics, vol. 13, no. 1, 2014, pp. 31–46., doi:10.1007/s12021-014-9238-1.

Sala-Llonch Roser, et al. “Evolving Brain Structural Changes in PSEN1 Mutation Carriers.” Neurobiology of Aging, vol. 36, no. 3, 2015, pp. 1261–1270., doi:10.1016/j.neurobiolaging.2014.12.022. [PubMed: 25638532]

Scahill Rachael I., et al. “Mapping the Evolution of Regional Atrophy in Alzheimer’s Disease: Unbiased Analysis of Fluid-Registered Serial MRI.” Proceedings of the National Academy of Sciences, vol. 99, no. 7, 2002, pp. 4703–4707., doi:10.1073/pnas.052587399.

Sepulcre Jorge, et al. “In Vivo Tau, Amyloid, and Gray Matter Profiles in the Aging Brain.” Journal of Neuroscience, vol. 36, no. 28, 2016, pp. 7364–7374., doi:10.1523/jneurosci.0639-16.2016. [PubMed: 27413148]

Shoup Timothy M., et al. “A Concise Radiosynthesis of the Tau Radiopharmaceutical, [18F]T807.” Journal of Labelled Compounds and Radiopharmaceuticals, vol. 56, no. 14, 2013, pp. 736–740., doi:10.1002/jlcr.3098. [PubMed: 24339014]

Sperling Reisa A., et al. “The Impact of Aβ and Tau on Prospective Cognitive Decline in Older Individuals.” Annals of Neurology, 2019, doi:10.1002/ana.25395.

Sperling Reisa A., et al. “Toward Defining the Preclinical Stages of Alzheimer’s Disease: Recommendations from the National Institute on Aging-Alzheimer’s Association Workgroups on Diagnostic Guidelines for Alzheimer’s Disease.” Alzheimer’s & Dementia, vol. 7, no. 3, 2011, pp. 280–292., doi:10.1016/j.jalz.2011.03.003.

Thompson Paul M., et al. “Dynamics of Gray Matter Loss in Alzheimer’s Disease.” The Journal of Neuroscience, vol. 23, no. 3, 2003, pp. 994–1005., doi:10.1523/jneurosci.23-03-00994.2003. [PubMed: 12574429]

Villemagne Victor L, et al. “Amyloid β Deposition, Neurodegeneration, and Cognitive Decline in Sporadic Alzheimer’s Disease: a Prospective Cohort Study.” The Lancet Neurology, vol. 12, no. 4, 2013, pp. 357–367., doi:10.1016/s1474-4422(13)70044-9. [PubMed: 23477989]

Wechsler David. WMS-R: Wechsler Memory Scale-Revised. Psychological Corporation, 1987.

Weston Philip S.J., et al. “Presymptomatic Cortical Thinning in Familial Alzheimer Disease.” Neurology, vol. 87, no. 19, 2016, pp. 2050–2057., doi:10.1212/wnl.0000000000003322. [PubMed: 27733562]

Xia Chenjie, et al. “Association of In Vivo [18F]AV-1451 Tau PET Imaging Results With Cortical Atrophy and Symptoms in Typical and Atypical Alzheimer Disease.” JAMA Neurology, vol. 74, no. 4, 2017, p. 427., doi:10.1001/jamaneurol.2016.5755. [PubMed: 28241163]

Yesavage Jerome A., et al. “Development and Validation of a Geriatric Depression Screening Scale: A Preliminary Report.” Journal of Psychiatric Research, vol. 17, no. 1, 1982, pp. 37–49., doi:10.1016/0022-3956(82)90033-4. [PubMed: 7183759]

HIGHLIGHTS

- Tau positron emission tomography images were acquired for 111 individuals.
- Magnetic resonance data were longitudinally collected (n_{scans}=386).
- Prospective structural changes were observed with higher inferior temporal tau.
- Lateral temporal regions may represent an inflection point in preclinical AD.
- Findings are consistent with the hypothesis that tau is a driver of atrophy.

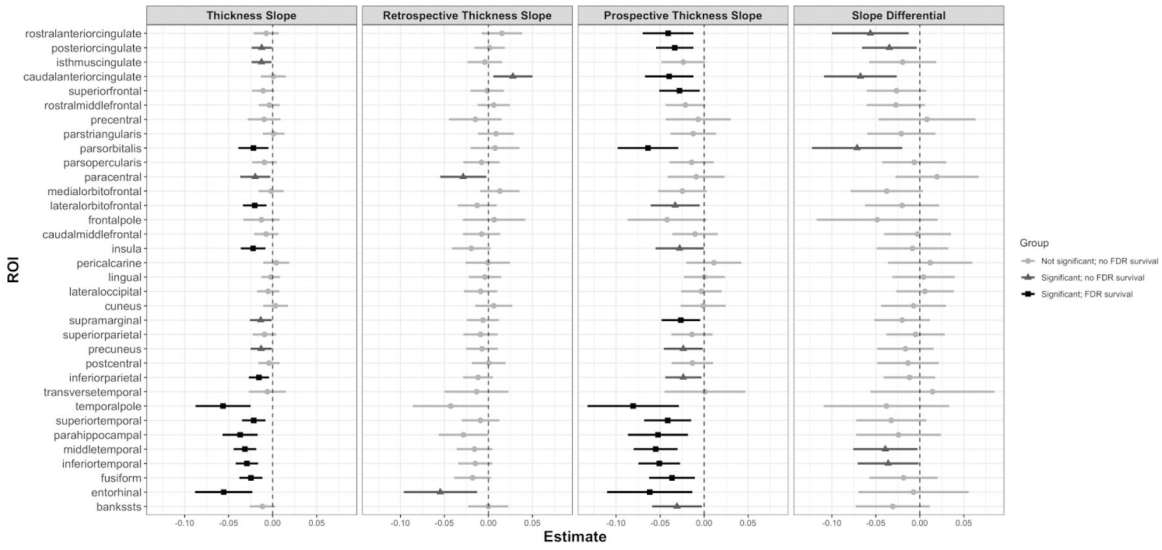

Fig. 1. IT FTP Effects

Forest plots for IT FTP analyses with lines centered at their respective unstandardized estimate with 95% confidence intervals. **Thickness Slope**) IT FTP × Time effect in Model 1, over the full observation period. **Retrospective Thickness Slope**) IT FTP:Time:G1 effect in Model 2B. **Prospective Thickness Slope**) IT FTP:Time:G2 effect in Model 2B. **Slope Differential**) IT FTP:Time:G effect in Model 2A, showing a comparison of retrospective versus prospective thickness slopes. Light gray indicates no significant effect, mild gray indicates a significant effect but no FDR survival, and black represents a significant effect with FDR survival. *Abbreviations*: FTP = flortaucipir; IT = inferior temporal gyrus; FDR = False Discovery Rate.

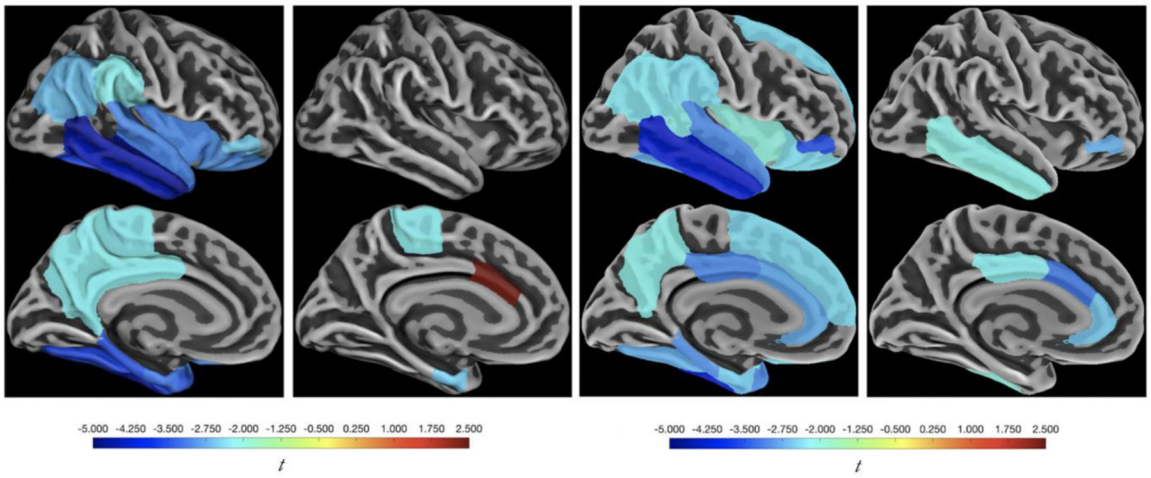

Fig. 2. Brain Maps of IT FTP Analyses

T-statistics from the effect of IT FTP on **(left most)** thickness over the full observation period, **(left middle)** retrospective thickness, **(right middle)** prospective thickness, and **(right most)** difference between retrospective and prospective thickness slopes are modeled as stated in Fig. 1 and Table 2. Only significant ROIs are shown, but they are not corrected for multiple comparisons. Bilateral measures were used for both SUVr and thickness. *Abbreviations*: FTP = flortaucipir; IT = inferior temporal gyrus; SUVr = standard uptake value ratios.

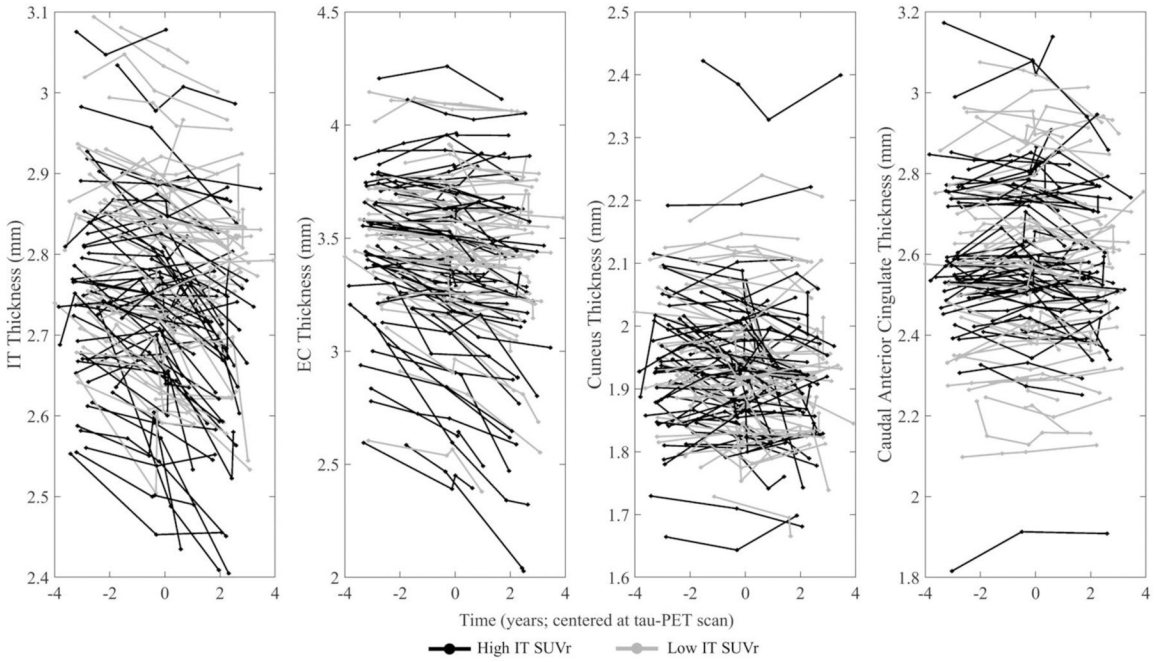

Fig. 3. Cortical Thickness Spaghetti Plots by High and Low IT FTP

IT FTP is stratified by a median IT SUVr of 1.46 (black = greater than 1.46, gray = less than or equal to 1.46) and longitudinal thickness data for all 111 participants are presented in the **(left most)** IT, **(left middle)** EC, **(right middle)** cuneus, **(right most)** caudal anterior cingulate. Data are centered at the tau-PET scan. Cuneus models were run with and without the uppermost individual shown, and no significant changes were found within full sample as well as amyloid group analyses. *Abbreviations*: IT = inferior temporal gyrus; EC = entorhinal cortex; SUVr = standardized uptake value ratio; FTP = flortaucipir.

4A. **Low PiB**

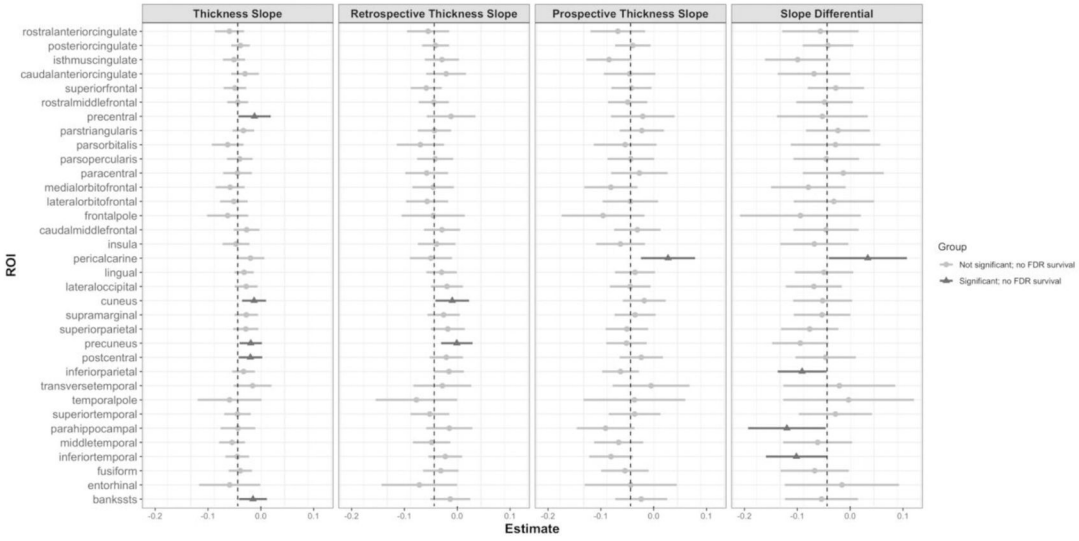

4B. **High PiB**

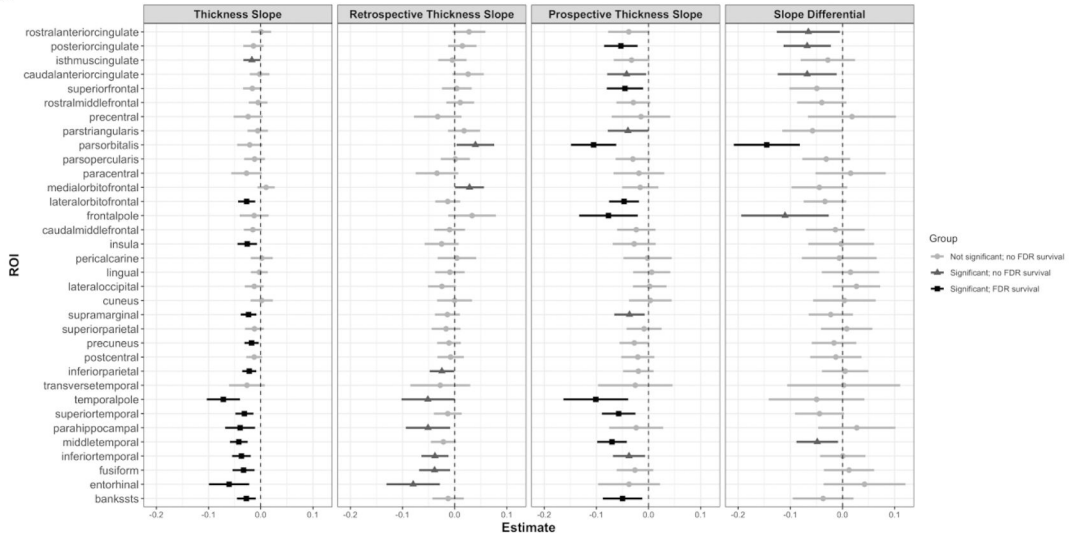

Fig. 4. IT FTP Effects in Low and High PiB Groups

Forest plots of LME estimates for all ROIs are shown, with the sample stratified by PiB group. Bars are centered at their respective beta estimate (unstandardized) with 95% confidence intervals. Moreover, light gray indicates no significant effect, mild gray indicates a significant effect but no FDR survival, and black represents a significant effect with FDR survival. *Abbreviations*: FTP = flortaucipir; IT = inferior temporal gyrus; EC = entorhinal cortex; PiB = Pittsburgh compound B; FDR = False Discovery Rate.

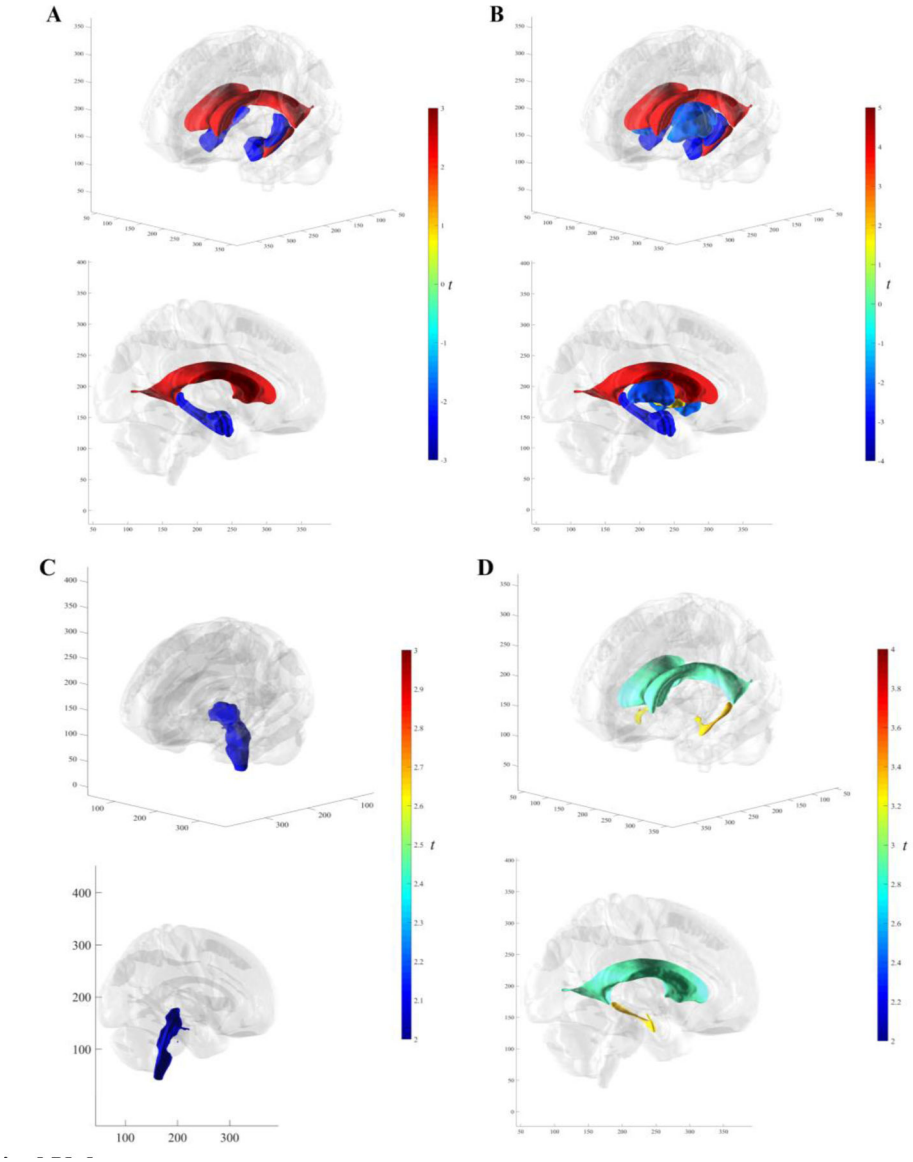

Fig. 5. Subcortical Volume

3D brain renderings of significant (no FDR correction) IT SUVr *t*-statistics. In order of increasing magnitude **(A)** Subcortical volume over the full follow-up range in the hippocampus, lateral ventricles, amygdala, and inferior lateral ventricles. **(B)** Prospective subcortical volume in the pallidum, putamen, thalamus proper, amygdala, hippocampus, lateral ventricles, and inferior lateral ventricles. **(C)** Retrospective subcortical volume in the brain stem. **(D)** Slope differences between retrospective and prospective thickness in the lateral and inferior lateral ventricles. *Abbreviations*: IT = inferior temporal gyrus; SUVr = standardized uptake value ratio; FTP = flortaucipir; FDR = False Discovery Rate.

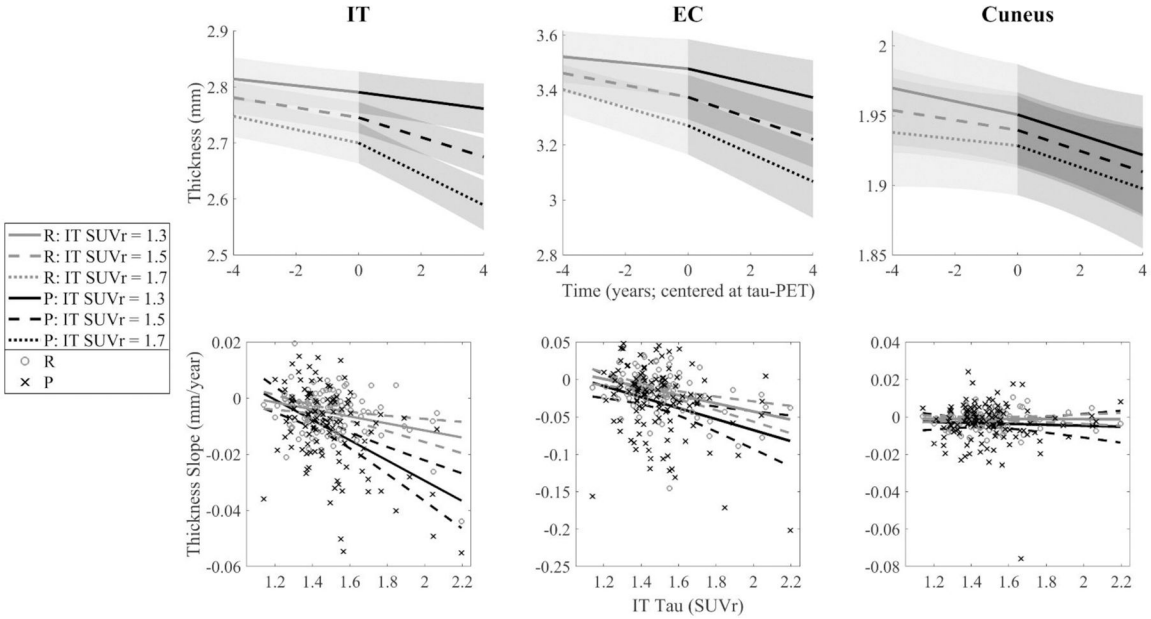

Fig. 6. The Influence of IT Tau on Cortical Thinning in Three Regions

(Top Row) IT, EC, and cuneus thinning are modeled at three levels of IT tau-PET (SUVr = 1.3, 1.5, and 1.7; median = 1.46) using estimates from Model 2A. **(Bottom Row)** Retrospective (gray *o*'s) and prospective (black *x*'s) thickness slopes are plotted against IT tau-PET signal. Slopes shown are representations of models analyzed, not direct reflections, as slopes were extracted by independent random effects of the equation: *Thickness* ~ 1 + (1|*Participant*) + (*Time*:*Retrospective Indicator* – 1|*Participant*) + (*Time*:*Prospective Indicator* – 1|*Participant*). *Abbreviations*: IT = inferior temporal gyrus; EC = entorhinal cortex; SUVr = standardized uptake value ratio; FTP = flortaucipir.

Table 1.

Demographic Information

	Aβ−	Aβ+	All	Uncorrected *p* value
N (% subsample)	72	35	111	--
Sex(*F*)	41 (56.94%)	19 (54.29%)	61 (54.95%)	0.83
*APOE*ε4+	13 (18.06%)	22 (62.86%)	37 (33.33%)	<0.001***
CDR = 0.5 at FTP session	5 (6.94%)	1 (2.86%)	6 (5.41%)	--
Mean (SD)				
Years of education	16.28 (3.06)	16.40 (2.83)	16.35 (2.98)	0.84
FTP session MMSE	29.39 (0.88)	29.03 (1.04)	29.25 (0.96)	0.06
FTP session Logical Memory (DR)	16.40 (3.97)	15.11 (3.31)	16.05 (3.79)	0.10
Number of MRI follow-up visits	3.55 (0.67)	3.33 (0.54)	3.48 (0.63)	0.10
MRI timespan (years)	4.36 (1.15)	4.59 (0.77)	4.46 (1.05)	0.32
Retrospective MRI timespan (years)	2.38 (0.94)	2.60 (0.81)	2.43 (0.90)	0.25
Prospective MRI timespan (years)	2.10 (0.80)	1.99 (0.64)	2.03 (0.78)	0.51
IT FTP SUVr	1.43 (0.12)	1.60 (0.23)	1.49 (0.19)	<0.001***
EC FTP SUVr	1.32 (0.22)	1.64 (0.41)	1.43 (0.33)	<0.001***
PiB DVR FLR	1.17 (0.07)	1.96 (0.42)	1.43 (0.45)	--

Participant information is presented at two levels of Aβ burden as well as in the full sample. Aβ group differences were computed using two sample t-tests, chi-squared tests, and were not corrected for multiple comparisons. Four participants did not have Aβ data. FTP and PiB data shown are partial volume corrected.

Key:

* $p<0.05$;

** $p<0.01$;

*** $p<0.001$;

Abbreviations: Aβ = beta-amyloid; *APOE*ε4 = Apolipoprotein E4 genotype; global Clinical Dementia Rating = CDR; Mini-Mental State Examination = MMSE; DR = delayed recall; FTP = flortaucipir; MRI = magnetic resonance imaging; IT = inferior temporal gyrus; EC = entorhinal cortex; SUVr = standardized uptake value ratio; PiB = Pittsburgh compound B; DVR = distribution volume ratio; FLR = frontolateral temporal/parietal-retrosplenial.

Table 2.

FTP Linear Mixed-Effect Models

Model 1	*Thickness* ~ *IT FTP* × *Time* + *Covariates* + (*Time*|*Participant*)
Model 2A	*Thickness* ~ *IT FTP* × *Time* × *G* - *G* - *IT FTP*:*G* + *Covariates* + (*Time*|*Participant*)
Model 2B	*Thickness* ~ *IT FTP*:*Time*:*G1* + *IT FTP*:*Time*:*G2* + *Time*:*G1* + *Time*:*G2* + *IT FTP* + *Covariates* + (*Time*|*Participant*)

Model 1) IT FTP by time interaction across all MR timepoints; **Model 2A**) To see slope differences in retrospective and prospective analyses, the two time periods are forced to have a shared intercept at time 0, which is achieved by including a three-way interaction with observation period (G) which codes whether an MR time point was obtained before or after FTP-PET, and then removing intercept terms G and IT FTP:G; **Model 2B**) Statistically equivalent to Model 2A, this was used to extract retrospective and prospective estimates directly. G1 is an indicator variable for the retrospective observation period and G2 is an indicator for the prospective observation period. *Note*: Wilkinson notation is used, '×' indicates an interaction with all combinations of lower-order terms, while ':' represents an interaction without lower-order terms (e.g., $x_1 \times x_2 \times x_3 = x_1{:}x_2{:}x_3 + x_1{:}x_2 + x_1{:}x_3 + x_2{:}x_3 + x_1 + x_2 + x_3$). As noted in the text, both models included ROI thickness as dependent variables, age and sex by time covariates, as well as random participant intercepts and random time slopes. *Abbreviations*: FTP = flortaucipir; IT = inferior temporal gyrus.